Synthesis, X-Ray Analysis, and Electrochemical Study of Some Manganese Carbonyl Derivatives with 1,1′-Bis(diphenylphosphino)ferrocene, dppfe

Satoru ONAKA,* Masa-aki HAGA,† Shigeru TAKAGI, Mayumi OTSUKA,†† and Katuya MIZUNO
Department of Chemistry, Nagoya Institute of Technology, Gokiso-cho, Showa-ku, Nagoya 466
† Department of Chemistry, Faculty of Education, Mie University, 1515 Kamihama, Tsu, Mie 514
†† Department of Applied Chemistry, Nagoya Institute of Technology, Gokiso-cho, Showa-ku, Nagoya 466
(Received March 23, 1994)

Synthesis and X-ray structure analyses were carried out for *fac-cis*-[MnCl(CO)$_3$dppfe] and *fac-cis*-[MnH(CO)$_3$dppfe], and a cyclic voltammetric study was made for a series of manganese carbonyl derivatives with 1,1′-bis(diphenylphosphino)ferrocene (dppfe), including these new compounds. Unusually a low oxidation potential for the Mn site is revealed for [Mn(MeCp)(CO)dppfe]. A good correlation between ν(CO) and the oxidation potential for the Mn atom has been clarified.

Metal complexes with an organometallic ligand, such as ferrocenylphosphines, are fascinating due to their potential as candidates for unusual magnetic and electrochemical properties owing to the presence of, and/or the cooperativity of, at least two different metal sites.[1,2] As to metal carbonyl complexes with a ferrocenylphosphine ligand, we have recently reported syntheses and X-ray molecular structure analyses of a series of metal carbonyl complexes with 1,1′-bis(diphenylphosphino)ferrocene (abbreviated to dppfe).[3] We have developed this chemistry while expecting a consequential interaction between the Fe in dppfe and the Mn or Co in the metal carbonyl moiety when these metals are located in close proximity. Although the distances between Fe and Mn, or Co, clarified by X-ray analyses for these complexes are beyond the scope of a significant interaction, quite interesting structural and spectral features have been revealed for [Mn(MeCp)(CO)dppfe]: the methyl substituent in MeCp and the CO on the manganese atom form an eclipsed conformation, and the CO stretching frequency appears at as low as 1810 cm^{-1} for a terminal carbonyl.[3] Recently, we succeeded in vidicating that this feature has occurred from the intramolecular C–H···OC–Mn interaction for the first time.[4] We have deemed that an increased electron density of the manganese atom should be responsible for this interaction, and should be reflected in the electrochemical behavior of this complex. We report here on an unusually low anodic potential in a cyclic voltammogram for this complex, compared with other manganese carbonyl complexes with dppfe.

Experimental

A series of manganese carbonyl derivatives, [Mn(MeCp)(CO)$_2$dppfe] (**1**), [Mn(MeCp)(CO)dppfe] (**2**), and [MnCl(CO)$_4$]$_2$(μ-dppfe) (**3**), was prepared according to a previous paper,[3] The synthetic procedure for *fac-cis*-[MnCl(CO)$_3$dppfe] (**4**), and *fac-cis*-[MnH(CO)$_3$dppfe] (**5**) are given in the following section.

[MnCl(CO)$_3$dppfe] (4). A toluene solution (50 mL) of $Mn_2(CO)_{10}$ (200 mg, 0.51 mmol) and dppfe (285 mg, 0.51 mmol) was refluxed under N_2 for 2.5 h. To the resulting brown solution was added 0.1 mL of CCl_4; the mixture was then refluxed for an additional 0.5 h. The dark-brown precipitates were filtered off, and the solvent was vacuum-stripped from the filtrate. An orange residue was subjected to column chromatography (silica gel). From a yellow fraction eluted with chloroform, the solvent was distilled off at reduced pressure, and the yellow product was recrystallized from CH_2Cl_2–hexane. Yield 120 mg (33%); ν(CO) (Nujol mull) 2024 (s), 1995 (s), 1929 (s) cm^{-1}; ^{31}P NMR ($CDCl_3$ soln) δ=47.7 (br) (H_3PO_4 standard).

[MnH(CO)$_3$dppfe] (5). A 1.5 mmol sample of $Mn_2(CO)_{10}$ (580 mg) and a 3.0 mmol sample of dppfe (1.66 g) were suspended into 80 mL of 1-propanol and the mixture was refluxed for 11 h. After cooled to room temperature, the resulting yellow precipitates were collected on a frit, washed with hexane (20 mL), and vacuum-dried to afford a yellow microcrystalline product **5**. Yield 1.55 g (74%). ν(CO) (Nujol mull) 1994 (vs), 1917 (vs), 1895 (vs) cm^{-1}; ^{31}P NMR ($CDCl_3$ soln) δ=77.3 (s) (H_3PO_4 standard); ^{1}H NMR δ=−6.13 (br. sing).

Electrochemical Measurement. Cyclic voltammetry was made at 20 °C with a BAS 100B/W and/or a BAS CV-50W electrochemical analyzer equipped with a platinum disk electrode for the working electrode and a platinum plate for an auxiliary electrode. A Ag/$AgNO_3$ (0.01 M) electrode was employed as the reference electrode with 0.1 M n-Bu_4NClO_4 (TBAP) or n-Bu_4NBF_4 (TBABF4) in acetonitrile (1 M=1 mol dm^{-3}). A Metrhom rotating-disk electrode assembly (model 628-10) was used for hydrodynamic voltammetry. Approximately a 10^{-3} M solution for each sample was prepared in dichloromethane and/or acetone, which contained 0.1 M TBAP or 0.1 M TBABF4 as a supporting electrolyte. A sweep rate of 200 mV s^{-1} was generally used for CV, except when otherwise noted. All of the manipulations were carried out under an argon atmosphere. The electrochemical data re tabulated in Table 1.

X-Ray Data Collection and Structure Determination. A yellow crystal of **4** with approximate dimensions of 0.50×0.20×0.10 mm^3 and yellow crystal of **5** with approximate dimensions of 0.25×0.25×0.10 mm^3 (both of which were grown from CH_2Cl_2–hexane) were mounted on a MAC MXC^3 diffractometer equipped with graphite monochromated Mo $K\alpha$ radiation (λ=0.71073 Å). The crystal data for these compounds are given in Table 2. The structure was solved by a direct method (MULTAN 78) and refined by a full-matrix least-squared method on a Sun SPARK2 work station (Crystan program system provided by MAC

Table 1. Voltammetric Data[a] and CO Stretching Frequencies

Compound	Conditions	1st oxidation			2nd oxidation			3rd oxidation			ν(CO)/cm^{-1} (Nujol)
		E_{pa}[b]	ΔE[c]	$E_{1/2}$[d]	E_{pa}	ΔE	$E_{1/2}$	E_{pa}	ΔE	$E_{1/2}$	
Mn(MeCp)(CO)$_2$dppfe (**1**)	CH_2Cl_2, 20 °C	+0.42	104	+0.37	+0.64	Irrev	Irrev	+0.80	Irrev	Irrev	1920, 1845
	CH_2Cl_2, −20 °C	+0.43	109	+0.38	+0.69	Irrev	Irrev				
Mn(MeCp)(CO)dppfe (**2**)	CH_2Cl_2, 20 °C	−0.31	82	−0.36	+0.76	Irrev	Irrev				1810
	CH_2Cl_2, −20 °C[e]	−0.29	138	−0.36	+0.78	155	+0.70				
[MnCl(CO)$_4$]$_2$(μ-dppfe) (**3**)	CH_2Cl_2, 20 °C	+0.80	230	+0.69	+1.02	210	+0.92				2095, 2028, 1960, 1919
MnCl(CO)$_3$dppfe (**4**)	CH_2Cl_2, 20 °C	+0.69	170	+0.61	+0.82	80	+0.78				2024, 1955, 1929
MnH(CO)$_3$dppfe (**5**)	CH_2Cl_2, 20 °C	+0.48	Irrev	Irrev	+0.78	140	+0.71				1994, 1917, 1895
	CH_2Cl_2, −20 °C	+0.52	180	+0.41	+0.75	96	+0.70				

a) a Platinum electrode (Ag/Ag$^+$ standard) with 0.1 M TBABF4 or TBAP at 100 mV scan rate. b) E_{pa}=anodic peak potential (V). c) ΔE=peak separation between anodic and cathodic peak potential (mV). d) $E_{1/2}$=half-wave potential (V). e) Scan rate=1 Vs^{-1}.

Table 2. Crystal Data

Compound	MnCl(CO)$_3$dppfe (**4**)	MnH(CO)$_3$dppfe (**5**)
Formula	$C_{37}H_{28}ClFeMnO_3P_2$	$C_{37}H_{29}FeMnO_3P_2$
Formula weight	727.99	694.03
Cryst system	Monoclinic	Triclinic
Space group	$P2_1/a$	$P\bar{1}$
a/Å	14.345 (3)	10.477 (2)
b/Å	19.388 (5)	17.463 (5)
c/Å	11.550 (3)	10.075 (3)
α/deg	90	105.59 (2)
β/deg	93.69(2)	115.50 (2)
γ/deg	90	75.36 (2)
V/Å^3	3206 (1)	1577.9 (7)
Z	4	2
d_{calcd}/g cm^{-3}	1.51	1.46
Cryst dimens/mm^3	0.50×0.20×0.10	0.25×0.25×0.10
μ(Mo $K\alpha$)/cm^{-1}	7.31	7.06
Scan type	ω–2θ	ω–2θ
Scan range/deg	1.34+0.5tanθ	1.0+0.35tanθ
Scan speed/deg min^{-1}	3	3
$2\theta_{max}$/deg	50	50
Unique reflections	5638	5552
Relfections with $\|F_o\|>3\sigma(\|F_o\|)$	3940	4010
No. of parameters refined	491	490
R	0.060	0.054
R_w	0.040	0.034

Temperature 24 °C; Mo $K\alpha$ radiation (λ=0.71073 Å); $R=\Sigma\|\|F_o\|-|F_c\|\|/\|F_o\|$; $R_w=[\Sigma w(\|F_o\|-\|F_c\|)^2/\Sigma w(F_o)^2]^{1/2}$ where $w=1/\sigma^2(F)$.

Science). Refinements were made anisotropically for non-hydrogen atoms and isotropically for hydrogen atoms. The molecular structures of **4** and **5** are shown in Fig. 1. The atomic coordinates are listed in Table 3, and selected bond lengths and angles are given in Table 4. The $|F_o|-|F_c|$ tables and anisotropic temperature factor tables are deposited as Document No. 67052 at the Office of the Editor of Bull. Chem. Soc. Jpn.

Spectral Measurements. The ^{1}H NMR spectra were measured with a Hitachi-Perkin-Elmer R-24B spectrometer (60 MH), and the ^{31}P NMR spectra were recorded with a Varian XL-200 spectrometer operated at 80.984 MHz in the Fourier-transform mode. The IR spectra were recorded on a JASCO 701G spectrometer and/or a JASCO Valor-III FT-IR spectrometer. The ν(CO) data are collated in Table 1.

Results and Discussion

Dppfe functions as a chelating ligand in **4** and **5**, similar to **2**. Both compounds assume a *fac-cis* structure. However, in the conformations determined by four phenyl groups, two phosphorus atoms, and the manganese atom are significantly different in the solid states for **4** and **5**, as can be seen from Fig. 1. The Mn–P bond lengths in **4** are significantly more elongated than those of **5**, and the Mn–Fe distance (4.445(1) Å) in **4** is also

Table 3. Atomic Coordinates and Equivalent Isotropic Thermal Parameters, B_{eq} (Å^2)

Atom	x	y	z	B_{eq}	Atom	x	y	z	B_{eq}
	[MnCl(CO)$_3$dppfe] (**4**)					[MnH(CO)$_3$dppfe](**5**)			
Mn	0.84116 (5)	0.12246 (4)	0.29429 (7)	2.71 (2)	Fe	0.83246 (7)	0.78770 (4)	0.46233 (8)	3.65 (3)
Fe	0.54586 (5)	0.10665 (4)	0.15476 (6)	2.73 (2)	Mn	0.91338 (8)	0.78842 (4)	0.92457 (8)	3.49 (3)
P 1	0.77587 (9)	0.08673 (7)	0.1086 (1)	2.41 (3)	P 1	0.9354 (1)	0.67838 (7)	0.7428 (1)	3.16 (4)
P 2	0.70690 (9)	0.09047 (7)	0.3966 (1)	2.48 (4)	P 2	0.7438 (1)	0.86891 (7)	0.7610 (1)	3.30 (4)
Cl	0.7805 (1)	0.23438 (7)	0.2501 (1)	4.28 (4)	C 1	0.7781 (5)	0.7652 (3)	0.9668 (5)	4.2 (2)
O 1	0.9349 (3)	−0.0093 (2)	0.3371 (4)	5.4 (1)	C 2	0.9536 (5)	0.8736 (3)	1.0722 (6)	4.8 (2)
O 2	0.9304 (3)	0.1795 (2)	0.5116 (4)	6.2 (2)	C 3	1.0628 (6)	0.7347 (3)	1.0552 (5)	4.6 (2)
O 3	1.0152 (3)	0.1746 (2)	0.2022 (4)	5.9 (2)	O 1	0.6923 (4)	0.7526 (2)	0.9984 (4)	7.0 (2)
C 1	0.8971 (4)	0.0396 (3)	0.3208 (5)	3.3 (2)	O 2	0.9860 (4)	0.9258 (2)	1.1730 (4)	7.6 (2)
C 2	0.8928 (4)	0.1566 (3)	0.4298 (5)	3.7 (2)	O 3	1.1612 (4)	0.7034 (2)	1.1433 (4)	6.8 (2)
C 3	0.9471 (4)	0.1531 (3)	0.2317 (5)	3.8 (2)	C 11	0.8824 (5)	0.6853 (2)	0.5473 (5)	3.3 (2)
C 11	0.6584 (3)	0.1140 (3)	0.0588 (4)	2.5 (1)	C 12	0.9780 (5)	0.6835 (3)	0.4786 (6)	4.2 (2)
C 12	0.6157 (4)	0.1802 (3)	0.0678 (5)	3.2 (2)	C 13	0.8977 (7)	0.6896 (3)	0.3276 (6)	5.5 (2)
C 13	0.5221 (4)	0.1754 (3)	0.0198 (5)	3.7 (2)	C 14	0.7506 (7)	0.6951 (3)	0.2980 (6)	4.9 (2)
C 14	0.5068 (4)	0.1080 (3)	−0.0188 (5)	3.3 (2)	C 15	0.7406 (5)	0.6918 (3)	0.4324 (5)	3.8 (2)
C 15	0.5891 (4)	0.0690 (3)	0.0034 (4)	2.9 (2)	C 16	0.7799 (5)	0.8808 (2)	0.6075 (5)	3.4 (2)
C 16	0.5903 (3)	0.0841 (3)	0.3233 (4)	2.6 (1)	C 17	0.9191 (5)	0.8844 (3)	0.6142 (6)	4.2 (2)
C 17	0.5286 (4)	0.1425 (3)	0.3194 (5)	3.4 (2)	C 18	0.9008 (6)	0.8911 (3)	0.4700 (6)	5.3 (2)
C 18	0.4416 (4)	0.1209 (4)	0.2651 (5)	4.3 (2)	C 19	0.7540 (6)	0.8919 (3)	0.3739 (6)	5.1 (2)
C 19	0.4483 (4)	0.0517 (4)	0.2354 (5)	4.0 (2)	C 20	0.6792 (5)	0.8863 (3)	0.4599 (6)	4.1 (2)
C 20	0.5391 (4)	0.0272 (3)	0.2699 (4)	3.1 (2)	C 21	1.1247 (5)	0.6305 (3)	0.7859 (5)	3.4 (2)
C 21	0.8450 (3)	0.1136 (3)	−0.0119 (4)	2.6 (1)	C 22	1.1673 (6)	0.5479 (3)	0.7787 (6)	4.2 (2)
C 22	0.8088 (4)	0.1536 (3)	−0.1020 (5)	3.5 (2)	C 23	1.3108 (6)	0.5159 (3)	0.8141 (6)	4.9 (2)
C 23	0.8617 (5)	0.1680 (4)	−0.1957 (5)	4.6 (2)	C 24	1.4129 (6)	0.5626 (4)	0.8513 (6)	5.1 (2)
C 24	0.9498 (5)	0.1413 (4)	−0.2004 (5)	4.6 (2)	C 25	1.3711 (6)	0.6444 (3)	0.8544 (6)	5.3 (2)
C 25	0.9878 (4)	0.1024 (4)	−0.1086 (5)	3.9 (2)	C 26	1.2278 (6)	0.6784 (3)	0.8259 (6)	4.8 (2)
C 26	0.9363 (4)	0.0884 (3)	−0.0150 (5)	3.5 (2)	C 31	0.8521 (5)	0.5926 (2)	0.7240 (5)	3.5 (2)
C 31	0.7682 (3)	−0.0066 (2)	0.0818 (4)	2.4 (1)	C 32	0.8572 (6)	0.5742 (3)	0.8523 (6)	4.7 (2)
C 32	0.7775 (4)	−0.0341 (3)	−0.0295 (5)	3.0 (2)	C 33	0.7994 (6)	0.5095 (4)	0.8445 (7)	5.8 (2)
C 33	0.7679 (4)	−0.1041 (4)	−0.0484 (6)	4.2 (2)	C 34	0.7315 (6)	0.4635 (3)	0.7081 (7)	6.0 (2)
C 34	0.7480 (4)	−0.1481 (3)	0.0417 (7)	4.3 (2)	C 35	0.7241 (6)	0.4809 (4)	0.5801 (6)	6.0 (2)
C 35	0.7386 (4)	−0.1218 (3)	0.1492 (5)	3.6 (2)	C 36	0.7856 (6)	0.5444 (3)	0.5883 (6)	4.8 (2)
C 36	0.7492 (4)	−0.0510 (3)	0.1702 (5)	2.8 (2)	C 41	0.5606 (4)	0.8436 (3)	0.6646 (5)	3.2 (2)
C 41	0.6755 (3)	0.1449 (3)	0.5182 (4)	2.7 (1)	C 42	0.5367 (5)	0.7656 (3)	0.6459 (5)	3.5 (2)
C 42	0.6255 (4)	0.1172 (3)	0.6052 (5)	4.3 (2)	C 43	0.3990 (6)	0.7464 (3)	0.5719 (6)	4.9 (2)
C 43	0.5951 (5)	0.1571 (4)	0.6942 (6)	5.0 (2)	C 44	0.2844 (6)	0.8042 (4)	0.5150 (6)	5.5 (2)
C 44	0.6149 (5)	0.2262 (4)	0.6982 (5)	4.9 (2)	C 45	0.3047 (5)	0.8814 (3)	0.5329 (6)	5.2 (2)
C 45	0.6615 (5)	0.2547 (3)	0.6124 (6)	4.8 (2)	C 46	0.4421 (5)	0.9008 (3)	0.6059 (6)	4.4 (2)
C 46	0.6935 (4)	0.2146 (3)	0.5221 (5)	3.9 (2)	C 51	0.7057 (5)	0.9740 (3)	0.8486 (5)	4.0 (2)
C 51	0.7291 (4)	0.0096 (2)	0.4774 (4)	2.8 (1)	C 52	0.6649 (6)	0.9895 (4)	0.9682 (6)	6.3 (2)
C 52	0.6762 (4)	−0.0499 (3)	0.4661 (5)	3.5 (2)	C 53	0.6312 (7)	1.0686 (5)	1.0349 (8)	8.0 (3)
C 53	0.7042 (5)	−0.1086 (3)	0.5311 (5)	4.4 (2)	C 54	0.6369 (7)	1.1306 (4)	0.979 (1)	8.6 (4)
C 54	0.7814 (5)	−0.1066 (3)	0.6072 (6)	4.6 (2)	C 55	0.6767 (7)	1.1169 (4)	0.8634 (9)	7.5 (3)
C 55	0.8312 (4)	−0.0476 (4)	0.6216 (6)	5.0 (2)	C 56	0.7114 (6)	1.0376 (3)	0.7963 (6)	5.1 (2)
C 56	0.8064 (4)	0.0099 (3)	0.5571 (6)	4.6 (2)	H 1	0.993 (4)	0.817 (2)	0.879 (4)	2.72 (0)
H 12	0.649 (4)	0.215 (3)	0.111 (5)	3.18 (0)	H 12	1.072 (5)	0.685 (3)	0.529 (5)	3.22 (0)
H 13	0.480 (4)	0.207 (3)	0.017 (5)	3.71 (0)	H 13	0.937 (5)	0.693 (3)	0.266 (5)	2.86 (0)
H 14	0.452 (4)	0.092 (3)	−0.049 (5)	3.30 (0)	H 14	0.671 (5)	0.695 (3)	0.204 (5)	2.95 (0)
H 15	0.595 (4)	0.021 (3)	−0.012 (5)	2.89 (0)	H 15	0.651 (5)	0.695 (3)	0.442 (5)	3.88 (0)
H 17	0.547 (4)	0.187 (3)	0.340 (5)	3.38 (0)	H 17	1.013 (5)	0.880 (3)	0.706 (5)	4.28 (0)
H 18	0.396 (4)	0.151 (3)	0.246 (5)	4.31 (0)	H 18	0.968 (6)	0.900 (3)	0.446 (6)	6.06 (0)
H 19	0.406 (4)	0.026 (3)	0.207 (5)	4.05 (0)	H 19	0.711 (6)	0.891 (4)	0.266 (6)	7.48 (0)

significantly longer than that of **5** (4.357(1) Å). These distances are far beyond the scope of a strong interaction between Fe and Mn.

Dppfe serves as a unidentate ligand in **1** and/or a trans bidentate ligand in **3**, although it functions as a chelating ligand in **2**, **4**, and **5**. However, the electrochemical behaviors for **1**, **3**, **4**, and **5** are similar; two or three anodic peaks are observed in the positive potential region. On the other hand, the cyclic voltammogram of **2** is quite different: one irreversible peak appears in the positive potential region and one reversible peak appears in the negative potential region

Table 3. (Continued)

Atom	x	y	z	B_{eq}	Atom	x	y	z	B_{eq}
H 20	0.566 (4)	−0.018 (3)	0.258 (5)	3.08 (0)	H 20	0.587 (5)	0.886 (3)	0.429 (5)	2.72 (0)
H 22	0.751 (4)	0.172 (3)	−0.100 (5)	3.51 (0)	H 22	1.097 (5)	0.518 (3)	0.760 (5)	3.22 (0)
H 23	0.837 (5)	0.193 (3)	−0.248 (5)	4.59 (0)	H 23	1.339 (5)	0.458 (3)	0.812 (5)	2.86 (0)
H 24	0.986 (4)	0.148 (3)	−0.264 (5)	4.60 (0)	H 24	1.513 (5)	0.538 (3)	0.876 (5)	2.95 (0)
H 25	1.042 (4)	0.089 (3)	−0.109 (5)	3.90 (0)	H 25	1.443 (5)	0.680 (3)	0.882 (5)	3.88 (0)
H 26	0.961 (4)	0.059 (3)	0.047 (5)	3.54 (0)	H 26	1.194 (5)	0.738 (3)	0.824 (5)	4.58 (0)
H 32	0.789 (4)	−0.010 (3)	−0.089 (5)	3.04 (0)	H 32	0.902 (5)	0.600 (3)	0.938 (5)	3.22 (0)
H 33	0.777 (4)	−0.121 (3)	−0.120 (5)	4.22 (0)	H 33	0.806 (5)	0.499 (3)	0.934 (5)	2.86 (0)
H 34	0.746 (5)	−0.189 (3)	0.031 (6)	4.35 (0)	H 34	0.693 (5)	0.426 (3)	0.712 (5)	2.95 (0)
H 35	0.720 (4)	−0.148 (3)	0.210 (5)	3.60 (0)	H 35	0.667 (5)	0.451 (3)	0.484 (5)	3.88 (0)
H 36	0.741 (4)	−0.035 (3)	0.250 (4)	2.82 (0)	H 36	0.771 (5)	0.554 (3)	0.496 (5)	4.58 (0)
H 42	0.608 (4)	0.073 (3)	0.603 (5)	4.29 (0)	H 42	0.613 (5)	0.727 (3)	0.685 (5)	3.22 (0)
H 43	0.560 (5)	0.144 (4)	0.743 (6)	5.00 (0)	H 43	0.386 (5)	0.692 (3)	0.556 (5)	2.86 (0)
H 44	0.592 (4)	0.248 (3)	0.755 (6)	4.89 (0)	H 44	0.191 (5)	0.789 (3)	0.462 (5)	2.95 (0)
H 45	0.674 (5)	0.293 (3)	0.611 (6)	4.81 (0)	H 45	0.223 (5)	0.923 (3)	0.501 (5)	3.88 (0)
H 46	0.725 (4)	0.235 (3)	0.454 (5)	3.87 (0)	H 46	0.449 (6)	0.952 (3)	0.624 (6)	4.58 (0)
H 52	0.616 (4)	−0.057 (3)	0.406 (5)	3.53 (0)	H 52	0.658 (5)	0.949 (3)	1.007 (6)	3.22 (0)
H 53	0.663 (4)	−0.148 (3)	0.520 (5)	4.35 (0)	H 53	0.608 (5)	1.074 (3)	1.123 (5)	2.86 (0)
H 54	0.804 (4)	−0.147 (3)	0.654 (5)	4.57 (0)	H 54	0.611 (5)	1.177 (3)	1.025 (5)	2.95 (0)
H 55	0.879 (4)	−0.045 (4)	0.673 (5)	5.03 (0)	H 55	0.676 (6)	1.157 (3)	0.822 (6)	3.88 (0)
H 56	0.835 (4)	0.050 (3)	0.573 (6)	4.65 (0)	H 56	0.738 (6)	1.032 (3)	0.722 (6)	4.58 (0)

Table 4. Selected Bond Lengths (Å) and Angles (°) for **4** and **5**

Compound **4**					
Bond lengths (Å)					
Mn–Cl	2.381 (2)	Mn–P_1	2.387 (1)	Mn–P_2	2.405 (2)
Mn–C_1	1.813 (6)	Mn–C_2	1.813 (6)	Mn–C_3	1.824 (6)
Fe–C_{11}	2.022 (5)	Fe–C_{12}	2.044 (6)	Fe–C_{13}	2.063 (6)
Fe–C_{14}	2.046 (5)	Fe–C_{15}	2.028 (5)	Fe–C_{16}	2.056 (5)
Fe–C_{17}	2.054 (6)	Fe–C_{18}	2.045 (6)	Fe–C_{19}	2.031 (6)
Fe–C_{20}	2.041 (6)	C_1–O_1	1.103 (7)	C_2–O_2	1.146 (7)
C_3–O_3	1.134 (7)				
Bond angles (°)					
Cl–Mn–P_1	87.41 (5)	Cl–Mn–P_2	92.71 (6)	P_1–Mn–P_2	94.95 (5)
C_1–Mn–C_2	91.5 (2)	C_1–Mn–C_3	89.1 (2)	C_2–Mn–C_3	85.3 (2)
Cl–Mn–C_1	174.5 (2)	Cl–Mn–C_2	88.6 (2)	Cl–Mn–C_3	85.4 (2)
Mn–C_1–O_1	176.8 (5)	Mn–C_2–O_2	175.5 (5)	Mn-C_3-O_3	173.8 (5)
Compound **5**					
Bond lengths (Å)					
Mn–H	1.34 (6)	Mn–P_1	2.313 (1)	Mn–P_2	2.303 (1)
Mn–C_1	1.800 (7)	Mn–C_2	1.786 (5)	Mn–C_3	1.789 (4)
Fe–C_{11}	2.042 (5)	Fe–C_{12}	2.048 (4)	Fe–C_{13}	2.050 (6)
Fe–C_{14}	2.032 (5)	Fe–C_{15}	2.027 (6)	Fe–C_{16}	2.011 (4)
Fe–C_{17}	2.050 (4)	Fe–C_{18}	2.075 (6)	Fe–C_{19}	2.065 (6)
Fe–C_{20}	2.031 (4)	C_1–O_1	1.157 (8)	C_2–O_2	1.158 (6)
C_3–O_3	1.156 (6)				
Bond angles (°)					
H–Mn–P_1	82 (2)	H–Mn–P_2	77 (2)	P_1–Mn–P_2	95.83 (5)
C_1–Mn–C_2	95.7 (3)	C_1–Mn–C_3	95.8 (3)	C_2–Mn–C_3	84.3 (2)
H–Mn–C_1	168 (2)	H–Mn–C_2	82 (2)	H–Mn–C_3	95 (2)
Mn–C_1–O_1	177.5 (4)	Mn–C_2–O_2	176.0 (4)	Mn–C_3–O_3	176.9 (4)

at room temperature (Fig. 2a). In order to clarify the electron transfer-processes for these waves, the following two voltammetries were attempted for **2**: (1) cyclic voltammetry at −20 °C and (2) rotating-disk voltammetry at −20 °C. Figures 2b, 2c, and 2d show cyclic, differential pulse, and rotating-disk voltammograms of **2**, respectively, in CH_2Cl_2 at −20 °C. Two reversible waves at $E_{1/2}=-0.36$ and 0.70 V vs. Ag/Ag^+ were observed. When the temperature was raised to 20 °C, a reversible response at 0.70 V collapsed into an irreversible one, preceded by a decrease in the ratio of the cathodic current vs. the anodic current for the first

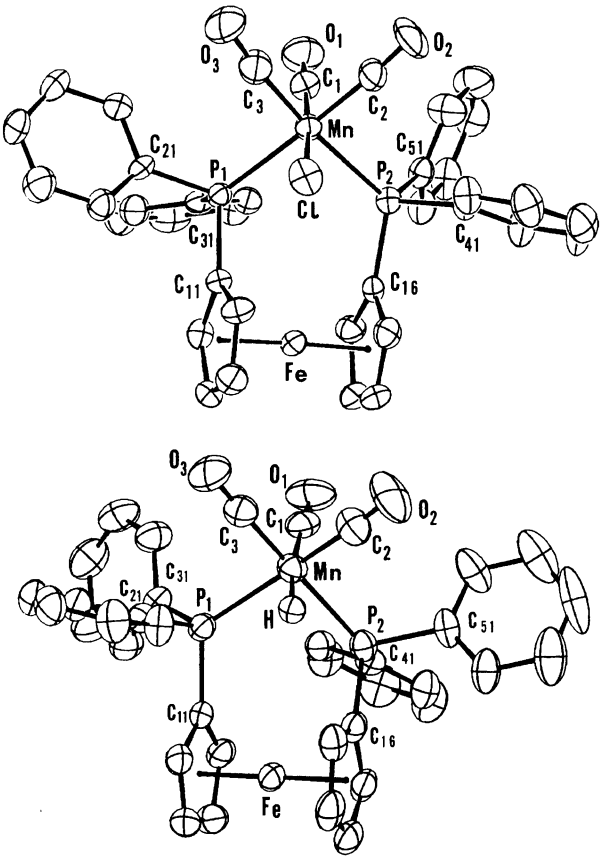

Fig. 1. Molecular structures of $MnCl(CO)_3dppfe$ (**4**) (upper) and $MnH(CO)_3dppfe$ (**5**) (lower).

process at −0.36 V. The rotating-disk voltammogram (Fig. 2d) revealed that these two waves correspond to oxidation processes (the current for each wave was at equal height). These data indicate that **2** exhibits essentially two one-electron oxidation processes. However, the species produced after the second oxidation is stable only at low temperature.[5)]

Complex **1** exhibits three anodic waves (I, II, and III) at room temperature. The first anodic wave exhibits a quasi-reversible behavior, i.e., the ratio of the anodic current vs. the cathodic current becomes close to 1 when the scan rate increases up to 1 $V\,s^{-1}$ (Fig. 3a insert). The second and third waves (II and III) are strongly temperature and scan-rate dependent. When the temperature was lowered to −20 °C, waves II and III coalesced into wave II (Fig. 3b). A rotating-disk voltammogram at −20 °C has revealed that the first (wave I) and second (wave II) processes are of equal height, which indicates that each process involves a one-electron transfer. Thus, waves I and II of **1** can be interpreted in terms of stepwise one-electron transfer processes. The low stability of the product formed by the second oxidation (wave II) for **1** seems to cause an irreversible behavior for the second oxidation process, even at low temperature. The following view seems to be tenable, that the species formed by the second oxi-

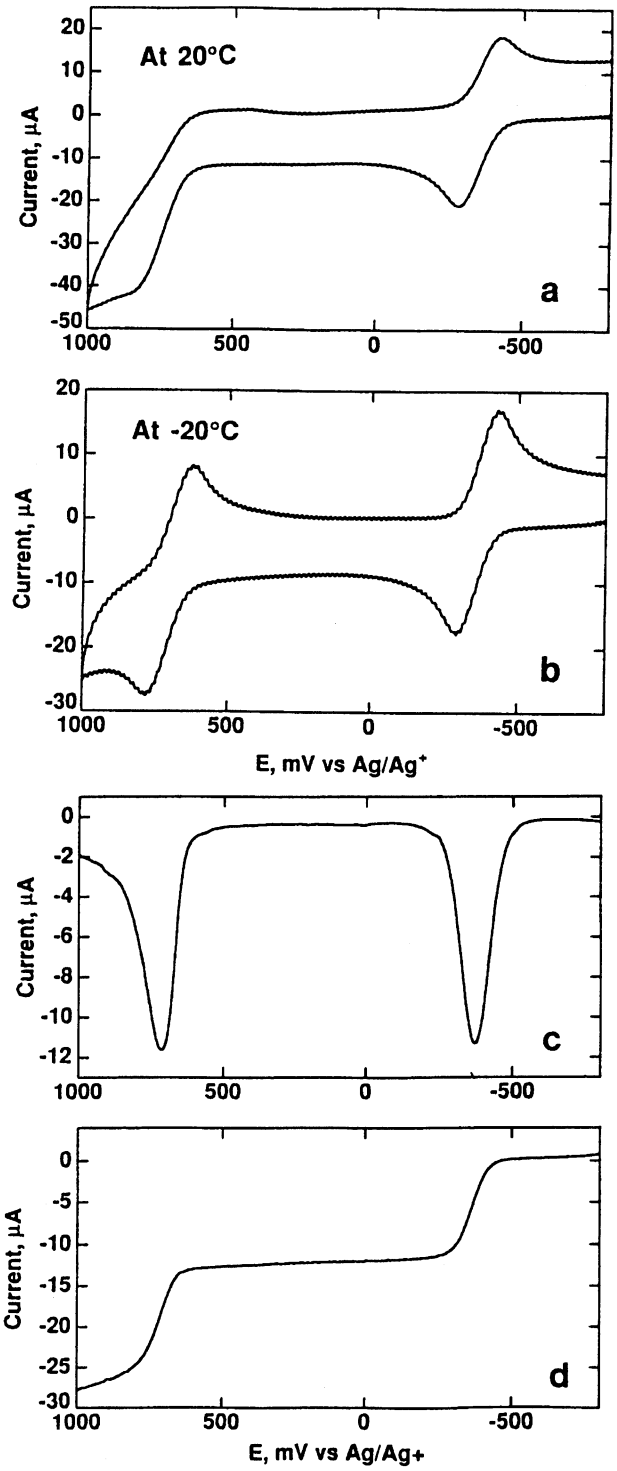

Fig. 2. Voltammograms of Mn(MeCp)(CO)dppfe (**2**) in CH_2Cl_2 (0.1 M TBABF4) with a platinum disk electrode. **a:** cyclic voltammogram at 20 °C with scan rate of 1 $V\,s^{-1}$. **b:** cyclic voltammogram at −20 °C with the same conditions as above. **c:** differential pulse voltammogram with scan rate of 4 $mV\,s^{-1}$ and pulse width 50 mV. **d:** rotating disk voltammogram with scan rate 20 $mV\,s^{-1}$ and rotation rate 1000 rpm.

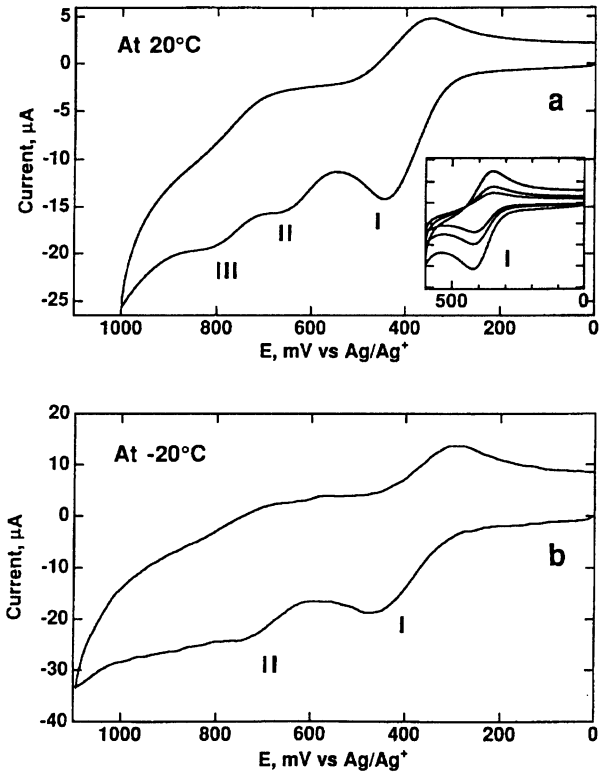

Fig. 3. Cyclic voltammogram of $Mn(MeCp)(CO)_2$-dppfe (**1**) in CH_2Cl_2 (0.1 M TBABF4). **a:** at 20 °C on a platinum disk electrode with scan rate=100 $mV\,s^{-1}$. Inserted Figure: scan rate 100, 200, and 500 $mV\,s^{-1}$. **2:** at −20 °C with the same conditions as above.

dation (wave II) decomposes more rapidly, and, thus, a new third oxidation wave (III) appears on a CV times scale when the temperature is raised to room temperature.

Compound **3** showed one reversible peak at $E_{1/2}$= 0.69 V and one quasi-reversible peak at $E_{1/2}$=0.92 V. Compound **4** showed one reversible peak at $E_{1/2}$=0.61 V and a quasi-reversible peak at $E_{1/2}$=0.78 V, while compound **5** showed a two-peak pattern for an anodic scan: an irreversible peak at E_{pa}=0.48 V and one reversible peak at E_{pa}=0.78 V. When the temperature was lowered to −20 °C, a completely irreversible peak at 0.48 V became quasi-reversible.

As can be seen from Table 1, all of these compounds exhibit an anodic peak at around E_{pa}=0.70 V. A literature survey of the dppfe–metal complexes has shown that the ferrocene-based oxidation waves (E_{pa}) are registered at around 0.70 V, referenced to the Ag/Ag^+ couple, and are not significantly influenced by the metal atom to which dppfe coordinates.[6—10] Similar potentials measured for all of the present compounds are consistent with the oxidation behavior for these ferrocene-based redox of dppfe–metal complexes.[6—10] When the E_{pa} data for the ferrocene-based oxidation are subtracted from Table 1, there remain E_{pa} data ranging from −0.31 to 1.02 V for the oxidation process on the manganese site. Along with a decrease in the electron density on the relevant metal site, it generally becomes more difficult to remove electrons from the metal atom, and the oxidation potential (E_{pa} and/or $E^{ox}_{1/2}$) should shift to a more a positive potential. Thus, the positive shift of the oxidation potential along with a change of a ligand other than dppfe means that the electron density on the manganese atom is decreased along with a change of the ligand. We previously showed that carbonyl stretching frequencies are quite sensitive to any change in the electron density on the manganese atom resulting in a shift to a higher energy along with a decrease in the electron density on the manganese atom for a series of X_3M–$Mn(CO)_5$ compounds.[11] Therefore, it is quite interesting to examine the correlation between the E_{pa} potential and the ν(CO) frequency. As demonstrated in Fig. 4, there indeed exists a good correlation between the symmetric CO stretching (A symmetry) frequency and the oxidation potential (E_{pa}) for the manganese site in each compound.[12] This correlation supports our selection of the E_{pa} peak for the manganese-based oxidation in each compound. The oxidation potential for the manganese atom in **2** seems to be unusually low. However, the oxidation-potential data for analogous manganese carbonyl derivatives, $CpMn(CO)(PPh_3)_2$ ($E_{1/2}$=−0.09 V vs. SCE)[13] and CpMn(CO)dppe ($E_{1/2}$=−0.16 V vs. SCE),[13,14] lend support to this assignment. The unusually low oxidation potential for the Mn site in **2** indicates that the electron density on the Mn site in **2** increases more than do those of **1**, **3**, **4**, and **5**. This pronounced increase in the elec-

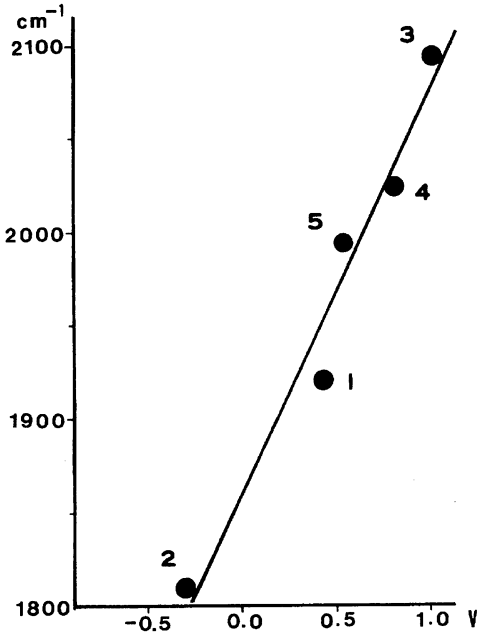

Fig. 4. Correlation between the E_{pa} potential for the Mn site and ν(CO) stretching frequency. The numbers in the graph represent the compounds in Table 1.

tron density on the Mn site should be responsible for the intramolecular C–H···OC–Mn interaction in **2**.[4)]

The present study was financially supported by a Grant-in-Aid for Science Research No. 05640627 from the Ministry of Education, Science and Culture and by The DAIKOU FOUNDATION. Thanks are also due to Dr. Hiroshi Nishihara of Keio University for his kind suggestion regarding CV measurements.

References

1) a) J. C. Kotz and C. L. Nivert, *J. Organomet. Chem.*, **52**, 387 (1973); b) J. C. Kotz, C. L. Nivert, and J. M. Lieber, *J. Organomet. Chem.*, **84**, 255 (1975); c) J. C. Kotz, C. L. Nivert, and J. M. Lieber, *J. Organomet. Chem.*, **91**, 87 (1975).

2) M. K. Loyd, J. A. McCleverty, D. G. Orchard, J. A. Connor, M. B. Hall, I. H. Hillier, E. M. Jones, and G. K. McEwen, *J. Chem. Soc., Dalton Trans.*, **1973**, 1743.

3) S. Onaka, *Bull. Chem. Soc. Jpn.*, **59**, 2359 (1986); S. Onaka, A. Mizuno, and S. Takagi, *Chem. Lett.*, **1989**, 2037; S. Onaka, T. Moriya, S. Takagi, A. Mizuno, and H. Furuta, *Bull. Chem. Soc. Jpn.*, **65**, 1415 (1992).

4) S. Onaka, H. Furuta, and S. Takagi, *Angew. Chem., Int. Ed. Engl.*, **32**, 87 (1993).

5) There are two conformers in solutions and these two conformers exchange rapidly at room temperature.[3,4)] This is the reason why one pair of CV data is available as an averaged data on the CV time scale.

6) M. Adachi, M. Kita, K. Kashiwabara, J. Fujita, N. Iitaka, S. Kurachi, S. Ohba, and D. -M. Jin, *Bull. Chem. Soc. Jpn.*, **65**, 2037 (1992).

7) S. Colbran, B. H. Robinson, and J. Simpson, *J. Chem. Soc., Chem. Commun.*, **1982**, 1361.

8) D. L. DuBois, C. W. Eigenbrot, Jr., A. Miedaner, J. C. Smart, and R. C. Haltwanger, *Organometallics*, **5**, 1405 (1986).

9) D. A. Clemente, G. Pilloni, B. Corain, B. Longato, and M. Tiripicchio-Camellini, *Inorg. Chim. Acta*, **115**, L9 (1986).

10) T. M. Miller, K. J. Ahmed, and M. S. Wrighton, *Inorg. Chim.*, **28**, 2347 (1989).

11) S. Onaka, *Bull. Chem. Soc. Jpn.*, **44**, 2135 (1971); S. Onaka, *Bull. Chem. Soc. Jpn.*, **46**, 2444 (1973); S. Onaka, *Nihon Kagaku Kaishi*, **1974**, 255.

12) A similar correlation has been reported for a series of $[Mn(\eta^5\text{-}C_5H_{5-n}Me_n)(CO)_{3-x}L_x]$ complexes and it has been clarified that E_{pa} data are most dependent on x rather than n and the nature of L.[13)] Although CO stretching frequency is most sensitive to the change of electron density on the relevant metal atom, CO stretching is also influenced to some extent by the nature of other ligand(s) especially the ligand in trans position on the relevant metal atom, which is called "trans effect". Significant deviation from linearity for some compounds in the present series of derivatives should be resulted from the "trans" influence of other ligand(s) than CO and dppfe on the (CO) data.

13) N. G. Connelly and M. D. Kitchen, *J. Chem. Soc., Dalton Trans.*, **1977**, 931.

14) L. I. Denisovich, N. V. Zakurin, S. P. Gubin, and A. G. Ginzuburg, *J. Organoment. Chem.*, **101**, C43 (1975).